Biophys. Struct. Mechanism 5, 293–312 (1979)

Biophysics of Structure and Mechanism

Molecular Mechanism for the Initial Process of Visual Excitation. IV. Energy Surfaces of Visual Pigments and Photoisomerization Mechanism

T. Kakitani

Department of Physics, Nagoya University,
Furo-cho, Chikusa-ku, Nagoya 464, Japan

Abstract. Using the twisted conformations of the chromophores for visual pigments and intermediates which were theoretically determined in the previous paper, energy surfaces of the pigment at −190° C were obtained as functions of the torsional angles θ_{9-10} and θ_{11-12} or of the torsional angles θ_{9-10} and θ_{13-14}. In these calculations, the existence of specific reaction paths between rhodopsin (R) and bathorhodopsin (B), between isorhodopsin I (I) and bathorhodopsin, and between isorhodopsin II (I′) and bathorhodopsin were assumed. It was shown that the total energy surfaces of the excited states had minima C_1 at $\theta_{9-10} \sim -10°$ and $\theta_{11-12} \sim -80°$, C_2 at $\theta_{9-10} \sim -85°$ and $\theta_{11-12} \sim -5°$, and C_3 at $\theta_{9-10} \sim 0°$ and $\theta_{13-14} \sim -90°$. These minima are considered to correspond to the thermally barrierless common states as denoted by Rosenfeld et al. Using the total energy surfaces in the ground and excited states, the molecular mechanism of the photoisomerization reaction was suggested. Quantum yields for the photoconversions among R, I, I′ and B were related to the rates of vibrational relaxations, radiationless transitions and thermal excitations. Some discussion was made of the temperature effect on the quantum yield. Similar calculations of the energy surfaces were also made at other temperatures where lumirhodopsin or metarhodopsin I is stable. Relative energy levels of the pigments and the intermediates were discussed.

Key words: Energy surfaces of visual pigments — Photoisomerization mechanism of visual pigments.

Introduction

In the preceding paper (Kakitani and Kakitani, 1979a), many of the specific properties of optical spectral data in visual pigments, their analogues and intermediates were consistently analyzed by assuming proper twisted conformations of chromophores based on the torsion model (Kakitani and Kakitani, 1975). The same model also predicted the barrierless energy surface in the excited state for the isomerization of the double bond (Kakitani and Kakitani, 1975).

0340-1057/79/0005/0293/$ 04.00

In this paper, we investigate the form of the interaction between the chromophore and opsin phenomenologically with inclusion of the solvent effect. For the purpose of this analysis, the previously calculated conformations of visual pigments and intermediates are fully used.

At present, it is not known what specific interactions between opsin and the chromophore are present. Our opinion is that the important part of the specific interaction will be the steric hindrance effect assisted by the induced fit mechanism of opsin. We can consider that the Coulombic interaction between the conjugated chain of the chromophore and some polar groups on opsin will work to some extent. But we think this latter effect will not work predominantly for the photoisomerization because the ionone ring of the chromophore is considered to be in a hydrophobic environment (Matsumoto and Yoshizawa, 1975), and then it will be difficult that ionized groups strongly interact with the ionone ring or conjugated bonds apart from the Schiff base bond.

Before going on our theme, we should like to express our opinion on some objections to the torsion model. The experiment by Mathies et al. (1977) showed that the resonance Raman spectra (RR spectra) of rhodopsin (R) and isorhodopsin (I) are very similar to those of 11-*cis* and 9-*cis* protonated retinylidene Schiff bases (PRSB's), respectively. From this, the chromophore conformations of R and I were considered to be not greatly different from those of the corresponding PRSB's (Mathies et al., 1977). It was also conjectured that the double bond of the chromophore would not be twisted (Callender and Honig, 1977; Aton et al., 1977). This is the first objection. As to this, we recently made a theoretical calculation, basing on the molecular orbital theory (Kakitani and Kakitani, 1979b). According to its result, the RR spectra of PRSB's are not so largely changed by twistings about double bonds as previously conjectured, and the calculated RR spectra of R and I using the twisted chromophore conformations which were obtained from the optical spectral analysis (Kakitani and Kakitani, 1979a) are roughly in agreement with those of 11-*cis* and 9-*cis* PRSB's, respectively. Therefore, the experimental results of the RR spectra of visual pigments can not preclude the possibility of the double bond twisting of the chromophore.

The second objection is why the double bond must be twisted in spite of the fact that there are many single bonds with small twisting force constants. As to this, we can show an example of the mechanism by which the double bond is selectively

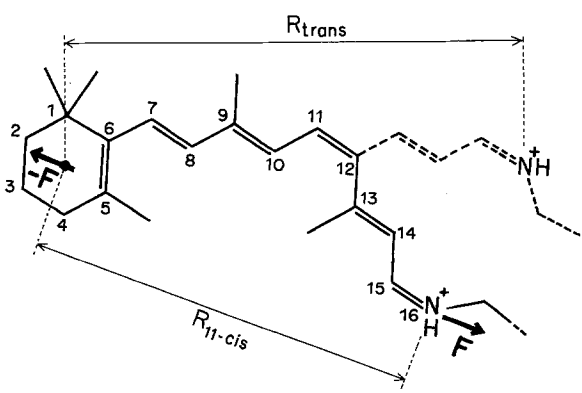

Fig. 1. Molecular structure of 11-*cis* protonated retinal Schiff base (PRSB). External force F is assumed to apply to the Schiff base nitrogen and the center of the ionone ring in the opposite direction

twisted. In Fig. 1, the molecular structure of the chromophore of R is drawn. We assume that the strain force $\mathfrak{F}$ is applied to the chromophore to enlarge the distance ($R_{11\text{-}cis}$) between the centre of the ionone ring and the nitrogen atom of the Schiff base in the protein moiety. It is evident that $R_{11\text{-}cis}$ is almost unchanged when the 7–8 double bond is twisted, and becomes a little large when the 9–10 and 13–14 double bonds are twisted, and becomes considerably large when the 11–12 double bond is twisted, whereas it decreases very much when any single bonds are twisted. Indeed, when the 11–12 double bond is isomerized, $R_{11\text{-}cis}$ becomes the largest (R_{trans}). Therefore, it is expected that the 11–12, 9–10, and 13–14 double bonds are twisted considerably under the operation of the strain force $\mathfrak{F}$. In order to examine this, we made a simple calculation as follows. The torsional energy V_t was assumed as

$$V_t = \sum_i^{\frac{1}{4}} K_i(1 - \cos 2\,\theta_i)\,, \tag{1}$$

where K_i and θ_i are the twisting force constant and the torsional angle of the i-th bond, respectively. K_i's corresponding to the double and single bonds are chosen to be 3.6 eV/rad^2 and 1.0 eV/rad^2, respectively, following the analysis by Tarasova and Sverdlov (1965) of vibrational frequencies of butadiene. Assuming a proper strain force $\mathfrak{F}$, we obtained $\theta_{11-12} \sim 20°$, $\theta_{9-10} \sim 20°$, $\theta_{10-11} \sim 17°$ and small angles for the other θ's. In this calculation, the correlation between twisting motions and bending motions of the conjugated chain due to steric hindrances among hydrogen atoms and methyl groups of the chromophore and nearby amino acid residues of opsin was taken into account. Then, it was concluded that the double bonds of the chromophore can be twisted considerably under the operation of the proper strain force to the chromophore. These mechanisms will be effective to the chromophore in the *cis* form. For the species with the chromophe of all-*trans* form such as bathorhodopsin, a different steric hindrance mechanism due to the unfitted conformation of the chromophore to the binding site of opsin will be important. The detail of the above investigation is to be published elsewhere (Kakitani, 1979).

The third objection will be the difficulty in explaining the large bathochromic shift of rhodopsin analogue formed from 11,12-dihydroretinal and opsin (Gawinowicz et al., 1977), in which the twisting of the small conjugated chain seems to be improbable. As to this, we discuss in the last section.

In the following sections, we investigate in more concrete form the interaction energy between the chromophore and opsin and the effect of solvation, but from a different point of view with use of the calculated conformations of the chromophores.

Total Energy of Visual Pigment

The total energy of a visual pigment E^T may be decomposed into three parts

$$E^T = E^O + E^C + E^I\,. \tag{2}$$

In this, E^O denotes the free energy of opsin with the protein conformation in the absence of the chromophore. E^C is the free energy of the chromophore. In the actual

calculation, we take account of only the π-electron energy and the molecular skeletal energy explicitly. The entropic term due to the molecular vibration of the chromophore is assumed to be constant for any chromophore conformation because most of the vibrational frequency is larger than kT and the vibrational quantum level occupied in each mode would be almost zero. The detailed calculation method for E^C is described later.

The interaction energy E^I includes the following terms;

$$E^I = E^H + E^E + E^S , \tag{3}$$

where E^H, E^E, and E^S are energies of steric hindrance, electronic Coulomb interaction, and solvation, respectively. The steric hindrance is due to the core-core repulsion between atoms or groups in very close proximity. E^E includes energies due to the Schiff base bonding, Coulombic interaction between the protonated Schiff base nitrogen and the counter anion which is believed to be located near the Schiff base, and to the nonsteric interaction between the hydrocarbon part of the chromophore and the protein moiety. It also includes all the electronic interactions among amino acid residues, peptide groups, hydrogen bond and so on caused by the change of the opsin conformation accompanying the binding of the chromophore. The solvation energy E^S is chiefly due to the hydrophobic interaction between the chromophore and solvent and hydrophyllic interaction between opsin and solvent.

The interaction energy E^I is dependent upon the temperature through E^E and E^S and it is dependent on the chromophore conformation through E^H, E^E, and E^S. In our analysis, E^I is considered to be the same for the ground and excited states of the chromophore.

The chromophore energy E^C is obtained by the self-consistent HMO theory (Kakitani, 1974; Kakitani and Kakitani, 1977) as follows.

$$E^C = 2\sum_a q_a\alpha_a + 2\sum_{(ab)} p_{ab}\beta^*_{ab} + \sum_{(ab)} f_{ab}(R_{ab}) + C , \tag{4}$$

$$\beta^*_{ab} = [\beta_{ab}(R_{ab}) - \zeta(2\,p_{ab} - \sum_{(cd)}^{\text{neigh.}} p_{cd}|\cos\theta_{cd}|)] \cdot |\cos\theta_{ab}| , \tag{5}$$

where q_a, α_a, p_{ab}, R_{ab}, θ_{ab}, f_{ab}, ζ, and C are electron charge density, Coulomb integral, bond order, bond length, torsional angle, skeletal bond energy, constant of the electron correlation energy and constant energy of the entropic contribution due to the molecular vibration. All the bond lengths and the π-electron state are solved self-consistently by minimizing E^C for each set of torsional angles.

In the present study we try to obtain E^I as a function of torsional angles of the chromophore.

Preliminary Calculations About Specific Reaction Paths

First of all, we assume that E^I consists of the hindrance potential at each bond as follows:

$$E^I = V_0 + \sum_{(ab)} \frac{1}{2} k_{ab}\,(\theta_{ab} - A_{ab})^2 + \cdots , \tag{6}$$

Table 1. Theoretical torsional angles in degree which were obtained previously for rhodopsin (R), isorhodopsin I (I), isorhodopsin II (I'), bathorhodopsin (B), lumirhodopsin (L), and metarhodopsin I (M). All the angles in this table are measured from the *trans* form. The other torsional angles θ_{5-6}, θ_{7-8}, and θ_{15-16} are zero

	θ_{6-7}	θ_{8-9}	θ_{9-10}	θ_{10-11}	θ_{11-12}	θ_{12-13}	θ_{13-14}	θ_{14-15}
R	−220	15	20	10	−152	25	0	15
I	−210	0	−157	25	25	20	0	15
I'	−210	15	−153	15	15	−25	−170	15
B	−230	−20	− 25	−30	− 38	−27	− 15	−15
L	−230	−15	25	15	− 26	30	15	15
M	−230	−30	20	15	29	22	0	15

where V_0, k_{ab} and A_{ab} are constants. At the equilibrium state,

$$\frac{\partial(E^C + E^I)}{\partial \theta_{ab}} = 0 . \tag{7}$$

Substituting Eqs. (4) and (6) into Eq. (7), we obtain

$$k_j(\theta_{ab} - A_{ab}) = 2\, p_{ab}\beta^*_{ab} \tan\theta_{ab} . \tag{8}$$

Given the values of θ_{ab}, p_{ab}, and β^*_{ab} for two species of the visual pigments and intermediates, we can evaluate k_{ab} and A_{ab}.

In Table 1, the torsional angles of the visual pigments and intermediates, which were determined for cattle in the previous study (Kakitani and Kakitani, 1979a), are listed. The numbering of the atom or bond is depicted in Fig. 1. All the torsional angles are measured from the *trans* form.

Using any two sets of θ_{ab}'s in Table 1, we can obtain k_{ab} and A_{ab} from Eq. (8). If the form of E^I in Eq. (6) is right for all the pigments, the calculated k_{ab} and A_{ab} should be the same for any two sets of θ's. However, the actual calculations did not show such a result. Thus, our assumption that the steric hindrance energy at each bond contributes to E^I independently is wrong. We must consider the steric hindrance potential which is correlated among torsional angles. For this purpose, we suppose that the energy surface of E^T will contain some definite reaction paths. That is, in the conversion between rhodopsin with an 11-*cis* form of the chromophore and bathorhodopsin with an all-*trans* form of the chromophore there may be a specific reaction path mainly along θ_{11-12}. Similarly, in the conversion from isorhodopsin I with a 9-*cis* form of the chromophore to bathorhodopsin there may be another specific reaction path mainly along θ_{9-10}. In the conversion from isorhodopsin II (I') with a 9,13-*dicis* form of the chromophore to bathorhodopsin there may be an other specific reaction path, mainly along θ_{9-10} and θ_{13-14}. Here, we assume that the steric hindrance energy near the reaction path could be expressed by the following.

$$E^I_r = V^r_0 + \sum_{(ab)} \frac{1}{2} k^r_{ab}(\theta_{ab} - A^r_{ab})^2 + \cdots , \tag{9}$$

where r denotes the species of the reaction path. Then the values of k^r_{ab} and A^r_{ab} calculated from Eq. (8) might be different for each reaction path.

Table 2. Calculated parameters of A^r (degree) and k^r (eV/rad^2) for the reaction paths between rhodopsin and bathorhodopsin (R ⇄ B), between isorhodopsin I and bathorhodopsin (I ⇄ B) and between isorhodopsin II and bathorhodopsin (I′ ⇄ B)

Reaction path	Bond													
	8–9		9–10		10–11		11–12		12–13		13–14		14–15	
	A^r	k^r	A^r	k^r	A^r	k^r	A^r	k^r	A^r	k^r	A^r	k^r	A^r	k^r
R ⇄ B	0	−1.5	0	−5.7	0	−2.0	−101	2.9	2	−2.1	0	−5.2	1	−2.3
I ⇄ B	−1	−1.6	−90	2.2	1	−1.9	−2	−5.1	2	−2.1	0	−5.2	1	−2.3
I′ ⇄ B	−1	−1.7	−87	2.3	0	−2.0	−2	−5.1	−20	−1.0	−104	0.9	1	−2.3

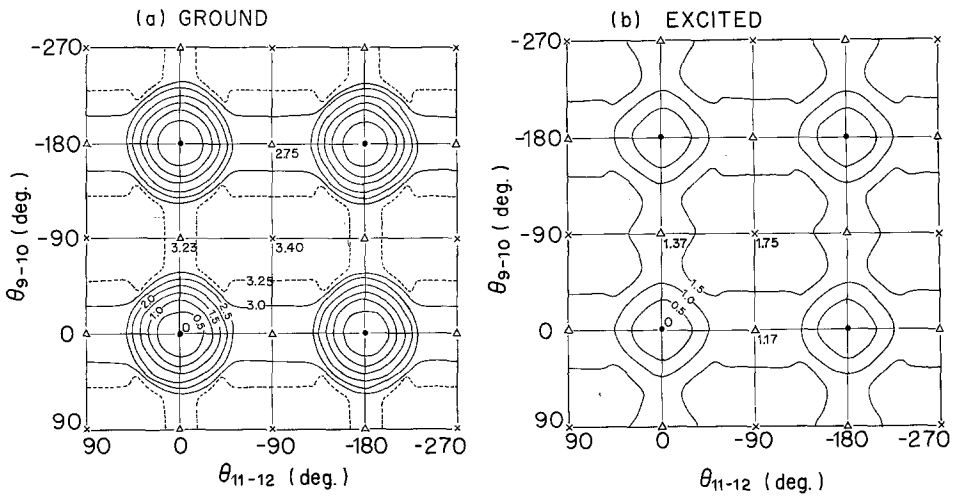

Fig. 2. Calculated energy surfaces of the chromophore energy E^C in the ground (**a**) and excited (**b**) states projected onto the $\theta_{9-10} - \theta_{11-12}$ plane. In this calculation, the torsional angles other than θ_{9-10} and θ_{11-12} are fixed to the absolute average values of R, B, and I. Symbols ●, △, and × denote minimum, saddle, and maximum, respectively. The unit of the energy contour line is eV. The origin of the energy is arbitrarily chosen at $\theta_{9-10} = \theta_{11-12} = 0°$

Under these considerations, we calculated k^r_{ab} and A^r_{ab} for the three reaction paths each of which connects with bathorhodopsin. The result is listed in Table 2. These values are considered as ones at liquid nitrogen temperature. From this, it is evident that there is a minimum of E^I_r at $\theta_{11-12} = -101°$ for the R ⇄ B reaction path, there is a minimum of E^I_r at $\theta_{9-10} = -90°$ for the I ⇄ B reaction path and there is a minimum of E^I_r at $\theta_{9-10} = -87°$ and $\theta_{13-14} = -104°$ for the I′ ⇄ B reaction path. It is also seen that the values of the other torsional angles are not largely different among the three reaction paths. The above results strongly support the assumption made in the torsion model that the interaction energy E^I will have a minimum near the transition states of the photoisomerization reactions. The negative value of k^r in Table 2 will not be important because higher order terms than the square form of Eq. (6) will become dominant and become positive for large value of $|\theta_{ab} - A^r_{ab}|$.

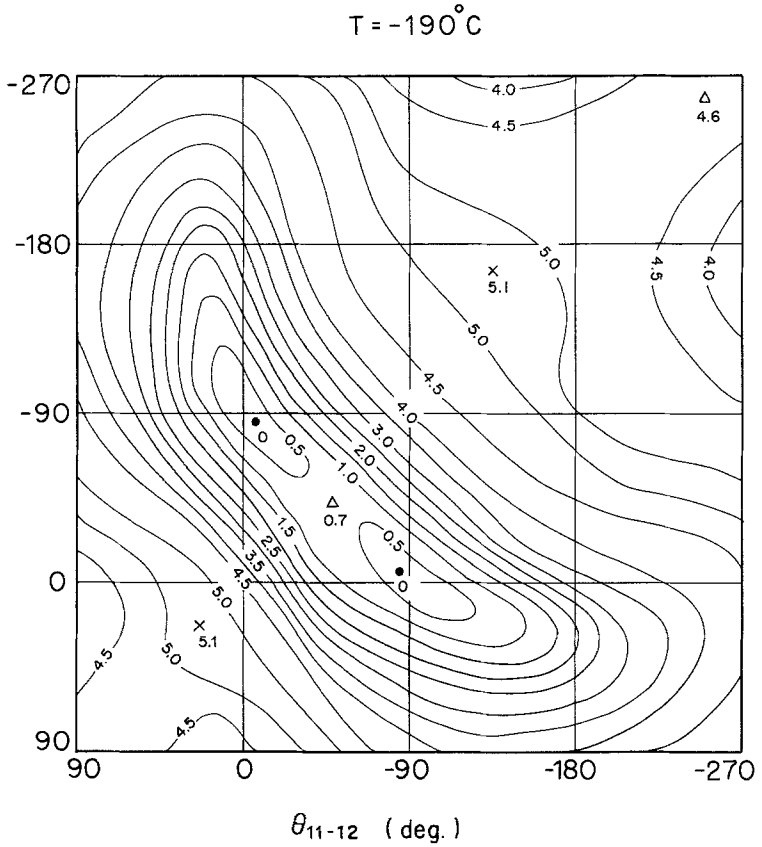

Fig. 3. The interaction energy surface E^I at $T = -190°$ C projected onto the $\theta_{9-10} - \theta_{11-12}$ plane. This energy map is estimated by the trial and error method so that the energy surface of $E^I + E^C$ in the ground state may have minima corresponding to R, B, and I at the torsional angles listed in Table 1. Symbols and unit are the same as Fig. 2

Energy Surfaces

In this section we calculate the energy surface of E^I and E^T projected onto the $\theta_{9-10} - \theta_{11-12}$ plane or the $\theta_{9-10} - \theta_{13-14}$ plane in detail, based on the results in the previous section. E^C is calculated by the self-consistent HMO theory (Kakitani and Kakitani, 1977). The torsional angles other than θ_{9-10} and θ_{11-12} (θ_{9-10} and θ_{13-14}) are replaced by the averages of the absolute values of ones for R, B, and I (I, B, and I′) listed in Table 1. The calculated E^C in the ground and excited states projected onto the $\theta_{9-10} - \theta_{11-12}$ plane are drawn in Fig. 2. It is evident that the hollow in the ground state is deeper than that in the excited state, and that wide plateaus exist in both the ground and excited states.

The interaction energy E^I as functions of θ_{9-10} and θ_{11-12} is obtained by the following process. First of all, we expect that E^I would have valleys along the reaction paths of R $\rightleftarrows$ B and B $\rightleftarrows$ I. Furthermore, the valley would have a minimum near

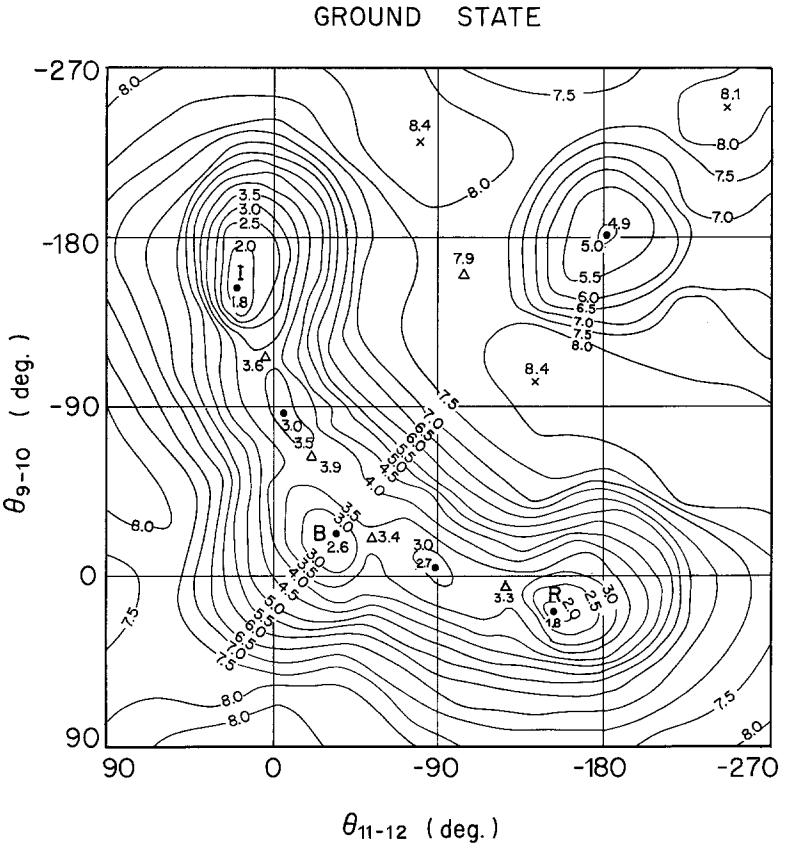

Fig. 4. The calculated total energy surface E^T of the ground state at $T = -190°$ C projected onto the $\theta_{9-10} - \theta_{11-12}$ plane. R, B, and I correspond to rhodopsin, bathorhodopsin, and isorhodopsin I, respectively. Other symbols and units are the same as Fig. 2

the transition state of the isomerization reaction, i.e., at $\theta_{9-10} \simeq 0°$ and $\theta_{11-12} \simeq -90°$ or at $\theta_{9-10} \simeq -90°$ and $\theta_{11-12} \simeq 0°$. Under these restrictions, we search the form of E^I in the $\theta_{9-10} - \theta_{11-12}$ plane by the trial and error method so that E^T may have minima at the values of θ_{9-10} and θ_{11-12} corresponding to R, B, and I as listed in Table 1. So obtained E^I is depicted in Fig. 3. Many of the energy contour lines run diagonally in the θ_{9-10} and θ_{11-12} plane. This demonstrates that the correlation between the two twistings around the 9—10 and 11—12 bonds is large in the reaction space of R $\rightleftarrows$ B $\rightleftarrows$ I. This energy contour map is obtained almost uniquely, especially near the minimum points.

The energy surface of E^T is obtained by adding Figs. 2 and 3. The result is shown in Figs. 4 and 5. From Fig. 4 we see that there are rather deep minima corresponding to R, B, and I and that there are two shallow minima near the transition states of isomerizations in the ground state. Figure 5 shows that two sharow minima C_2 and C_3 exist at $\theta_{9-10} = -10°$, $\theta_{11-12} = -80°$, and at $\theta_{9-10} = -85°$, $\theta_{11-12} = -5°$, respectively, in the excited state. Narrow and deep valleys extend along the

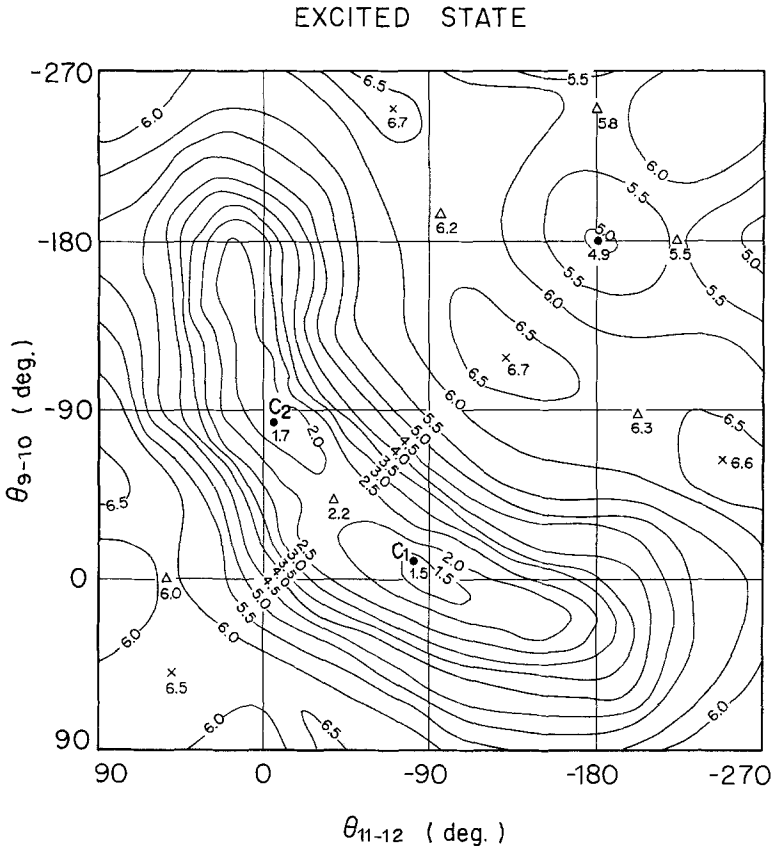

Fig. 5. The calculated total energy surface E^T of the excited state at $T = -190°$ C projected onto the $\theta_{9-10} - \theta_{11-12}$ plane. C_1 and C_2 would correspond to the common state denoted by Rosenfeld et al. Other symbols and unit are the same as Fig. 2

reaction paths. This property will be useful in showing that the direction of the isomerization of the visual pigment is exceedingly specific.

Similarly, in obtaining E^I in the $\theta_{9-10} - \theta_{13-14}$ plane for the conversion among I, B, and I′, we pose the restriction that E^I would have valleys along the reaction paths of I $\rightleftarrows$ B and B $\rightleftarrows$ I′, and that the valley would have minima near the transition states, i.e., at $\theta_{9-10} \simeq -90°$ and $\theta_{13-14} \simeq 0°$, and at $\theta_{9-10} \simeq -90°$ and $\theta_{13-14} \simeq -90°$. The energy surface of E^C in the $\theta_{9-10} - \theta_{13-14}$ plane is calculated by the same method as before, and the results are somewhat similar to those of Fig. 2. Under these conditions, we search the potential form of E^I in the $\theta_{9-10} - \theta_{13-14}$ plane by the trial and error method so that E^T may have minima at the values of θ_{9-10} and θ_{13-14} corresponding to I, B, and I′ as listed in Table 1. So obtained E^I is depicted in Fig. 6. This form of E^I is considerably different from that of Fig. 3 except for the region near the reaction path I $\rightleftarrows$ B. Many of the energy contour lines in Fig. 6 run diagonally in the θ_{9-10} and θ_{13-14} plane. Thus, the correlation between θ_{9-10} and θ_{13-14} is large also in the conversion space of I $\rightleftarrows$ B $\rightleftarrows$ I′.

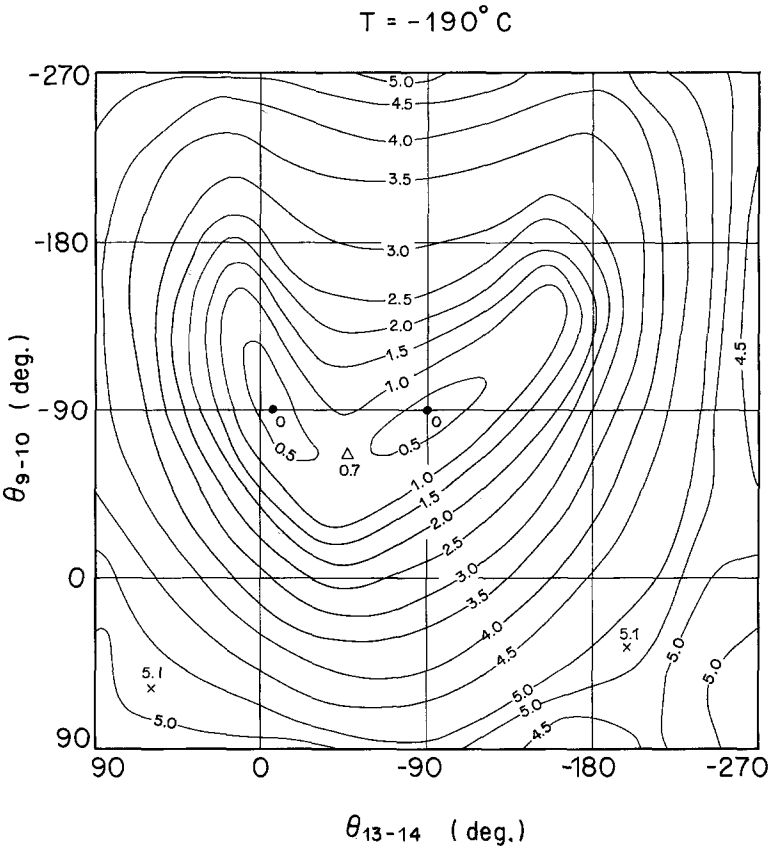

Fig. 6. The interaction energy surface E^I at $T = -190°$ C projected onto the $\theta_{9-10} - \theta_{13-14}$ plane. This energy map is estimated by the trial and error method that the energy surface of $E^I + E^C$ may have minima in the ground state corresponding to I, B, and I′ at the torsional angles listed in Table 1. Symbols and unit are the same as Fig. 2

Photoisomerization Mechanism

Combining Figs. 4 and 5, we obtain Fig. 7. Two shallow minima in the ground state are named D_1 and D_2. These correspond to the transition states in the thermal isomerization reactions R $\rightleftarrows$ B and I $\rightleftarrows$ B, respectively. Similarly, the combined energy surfaces in the $\theta_{9-10} - \theta_{13-14}$ plane are depicted in Fig. 8. In this case there are three deep minima in the ground state corresponding to I, B, and I′. There also appear two shallow minima D_2 and D_3 which are the transition states in the thermal isomerizations I $\rightleftarrows$ B and B $\rightleftarrows$ I′, respectively. In the excited state, two minima C_2 and C_3 appear at $\theta_{9-10} = -85°$, $\theta_{13-14} = -10°$ and at $\theta_{9-10} = -90°$, $\theta_{13-14} = -90°$, respectively.

Using Figs. 7 and 8, one can imagine the reaction path of the photoconversion among R, B, I, and I′ as follows. By absorbing a light quantum, R is excited to the Franck-Condon state F_r, followed by the rapid vibrational relaxation to C_1. Then, the radiationless transitions $C_1 \rightarrow D_1$, $C_1 \rightarrow$ B, and $C_1 \rightarrow$ R will occur. The one

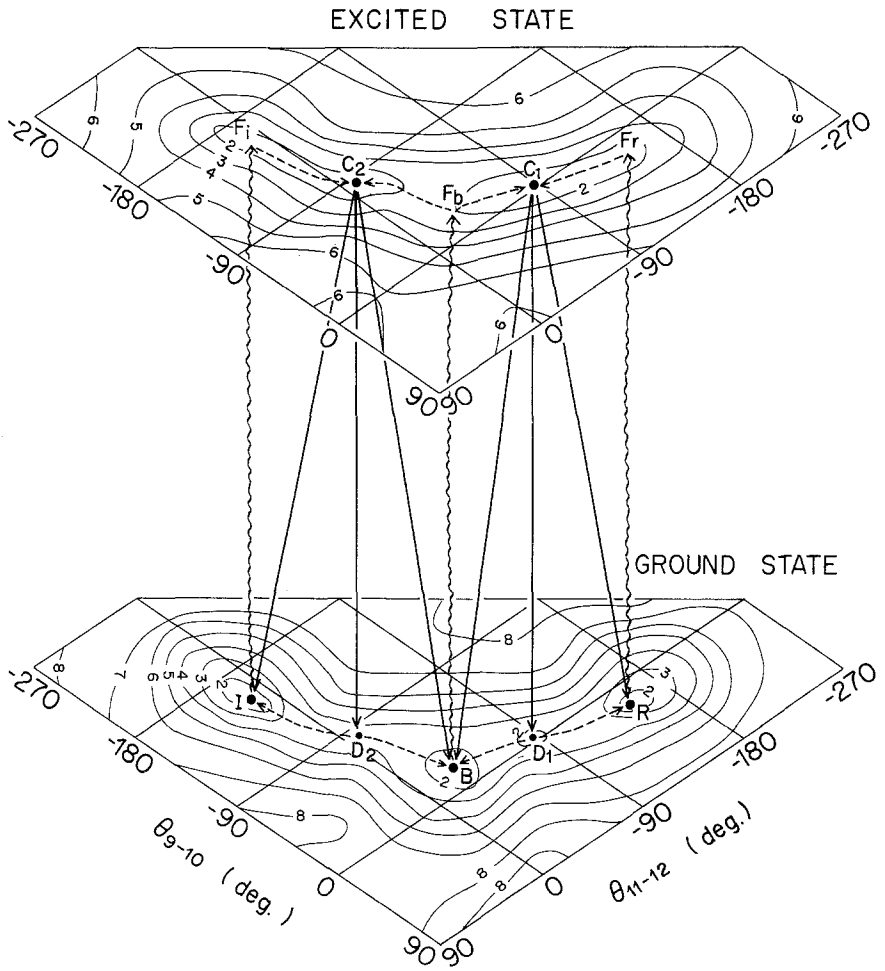

Fig. 7. Photoreaction scheme in the $\theta_{9-10} - \theta_{11-12}$ plane with use of the energy surfaces of Figs. 4 and 5. R, B, and I are the same notation as Fig. 4. D_1 and D_2 are small minima in the ground state. F_r, F_b, and F_i are the Franck-Condon states excited from R, B, and I, respectively. $C_1$and C_2 are the same notation as Fig. 5. ⟿ denotes the photo-excitation process, - - - → the relaxation process and ——→ the radiationless transition process. The other symbols and unit are the same as Fig. 2

reaching D_1 transforms to the more stable species R or B by a thermal excitation.

When I absorbs a photon, I is excited to the Franck-Condon state F_i, followed by the rapid relaxation to C_2. Then, there will be four roots of radiationless transitions $C_2 \rightarrow D_2$, $C_2 \rightarrow$ B, $C_2 \rightarrow$ R, and $C_2 \rightarrow D_3$. The one reaching D_2 will go to B or I and the one reaching D_3 to B or I′ by thermal excitations. In this, the radiationless transition rate of $C_2 \rightarrow D_3$ is considered to be fairly slow compared with those of $C_2 \rightarrow$ B and $C_2 \rightarrow$ R because the difference of chromophore conformations between C_2 and D_3 is large while its energy gap is small.

When I′ absorbs a light quantum, it is excited to the Franck-Condon state F_i, and it rapidly relaxes to C_3. Then, the radiationless transition $C_3 \rightarrow D_3$ will occur

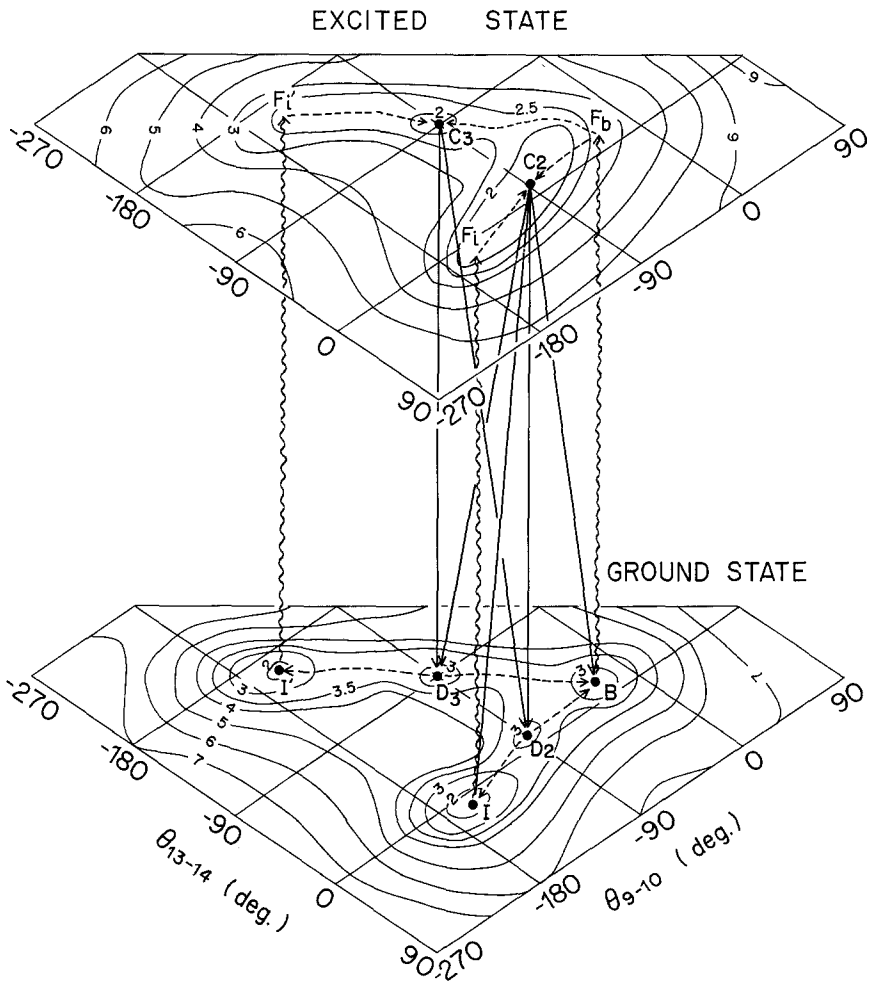

Fig. 8. Photoreaction scheme in the $\theta_{9-10} - \theta_{13-14}$ plane. B, I, F_b, and F_i are the same as Fig. 7. I′ is isorhodopsin II. D_3 is the small minimum in the ground state. F_i' is the Franck-Condon state excited from I′. C_3 is the common state between F_b and F_i'. All the other notations and unit are the same as Fig. 7

dominantly compared with the transition $C_3 \rightarrow D_2$ by the same reason as the transition $C_2 \rightarrow D_3$. The one reaching D_3 proceeds to B or I′ and the one reaching D_3 to I by thermal excitations.

When B absorbs a light quantum, it is raised to the Franck-Condon state F_r, followed by a rapid vibrational relaxation to C_1, C_2 or C_3. In this, the rate of the relaxation $F_b \rightarrow C_3$ is thought to be much smaller than those of $F_b \rightarrow C_1$ or $F_b \rightarrow C_2$, owing to the long relaxation process as seen in Fig. 8. The succeeding processes to these states are the same as before.

According to these photoisomerization mechanisms, there is no direct reaction path connecting F_i with F_r. Therefore, the isomerization of R $\rightleftarrows$ I due to a single photon absorption hardly occurs, in qualitative agreement with the result of the

kinetic analysis (Sarai et al., 1979). In contrast with this, the simultaneous isomerization of the 9–10 and 13–14 double bonds by a single photon absorption is possible in the conversion I′ → B.

Quantum Yield

The quantum yields γ'_s of the photoisomerization among R, I, I′, and B are written by the transition rates k's as follows.

$$\gamma_{R\to B} = \frac{k_{C1\to B}}{k_1} + \frac{k_{C1\to D1}}{k_1}\cdot\frac{K_{RB}}{1+K_{RB}}, \tag{10}$$

$$\gamma_{B\to R} = \frac{1}{1+a}\left[\frac{k_{C1\to R}}{k_1} + \frac{k_{C1\to D1}}{k_1}\cdot\frac{1}{1+K_{RB}}\right], \tag{11}$$

$$\gamma_{I\to B} = \frac{k_{C2\to B}}{k_2} + \frac{k_{C2\to D2}}{k_2}\cdot\frac{K_{IB}}{1+K_{IB}}, \tag{12}$$

$$\gamma_{B\to I} = \frac{a}{1+a}\left[\frac{k_{C2\to I}}{k_2} + \frac{k_{C2\to D2}}{k_2}\cdot\frac{1}{1+K_{IB}}\right], \tag{13}$$

$$\gamma_{I'\to B} = \frac{k_{C3\to D3}}{k_3}\cdot\frac{K_{I'B}}{1+K_{I'B}} + \frac{k_{C2\to D2}}{k_2}\cdot\frac{K_{IB}}{1+K_{IB}}, \tag{14}$$

$$\gamma_{B\to I'} = \frac{a}{1+a}\cdot\frac{k_{C2\to D3}}{k_2}\cdot\frac{1}{1+K_{I'B}}, \tag{15}$$

where

$$\begin{aligned}
k_1 &= k_{C1\to D1} + k_{C1\to B} + k_{C1\to R},\\
k_2 &= k_{C2\to D2} + k_{C2\to B} + k_{C2\to I} + k_{C2\to D3},\\
k_3 &= k_{C3\to D3} + k_{C3\to D2},\\
a &= k_{Fb\to C2}/k_{Fb\to C1},\\
K_{RB} &= k_{D1\to B}/k_{D1\to R},\\
K_{IB} &= k_{D2\to B}/k_{D2\to I},\\
K_{I'B} &= k_{D3\to B}/k_{D3\to I'},
\end{aligned} \tag{16}$$

and the small rate process $F_b \to C_3$ is neglected.

It is a significant problem to evaluate these transition rates. For this purpose, it will be necessary to determine the energy surfaces more unambiguously, especially for the thermal excitation processes. According to our preliminary calculations using

the energy surfaces obtained in this study and applying the Jortner's theory (1976) as to the nonadiabatic multivibration decay process to our case, the radiationless transition rate of $C_1 \rightarrow D_1$ was comparable with or smaller than those of $C_1 \rightarrow$ B and $C_1 \rightarrow$ R (Kakitani et al., 1979).

Recent experimental results by Hurley et al. (1977) showed that $\gamma_{R \rightarrow B}$ is independent of temperature (at least from $-196°$ C to 25° C) while $\gamma_{I \rightarrow B}$ is considerably dependent upon temperature. Furthermore, $\gamma_{B \rightarrow R}$ at $-196°$ C (Strackee, 1972) is similar to $\gamma_{M \rightarrow R}$ at $-20°$ C (Kropf and Hubbard, 1958). We should like to consider that the latter fact implies the temperature independence of $\gamma_{B \rightarrow R}$. From these experimental results we can derive the following properties. Assuming that the thermal equilibrium is attained immediately after the radiationless transition $C_1 \rightarrow D_1$, one can write K_{RB} as

$$K_{RB} = \exp\left[-(E^{\neq}_{D1 \rightarrow R} - E^{\neq}_{D1 \rightarrow B})/RT\right], \tag{17}$$

where $E^{\neq}_{D1 \rightarrow R}$ and $E^{\neq}_{D1 \rightarrow B}$ are the transition state energies in the thermal conversions from D_1 to R and from D_1 to B, respectively. It is improbable that $E^{\neq}_{D1 \rightarrow R}$ is the same as $E^{\neq}_{D1 \rightarrow B}$. So that K_{RB} has a temperature dependence. Therefore, for $\gamma_{R \rightarrow B}$ and $\gamma_{B \rightarrow R}$ to be independent of temperature, the second term in Eqs. (10) and (11) should be smaller than the first term (i.e., $k_{C1 \rightarrow D1}$ should be considerably smaller than $k_{C1 \rightarrow B}$ and $k_{C1 \rightarrow R}$) Then, we can approximate Eqs. (10) and (11) as

$$\gamma_{R \rightarrow B} \simeq \frac{b}{1+b}, \tag{18}$$

$$\gamma_{B \rightarrow R} \simeq \frac{1}{1+a} \cdot \frac{1}{1+b}, \tag{19}$$

where

$$b = k_{C1 \rightarrow B}/k_{C1 \rightarrow R}. \tag{20}$$

From Eq. (18), b should be independent of temperature. In general, the radiationless transition rate depends upon temperature. Thus, it is rather surprising that b is independent of temperature. That is, the temperature dependence of $k_{C1 \rightarrow B}$ should be quite similar to that of $k_{C1 \rightarrow R}$.

For $\gamma_{I \rightarrow B}$ to be dependent on temperature, there are some ways. One is $k_{C2 \rightarrow D2} \gg k_{C2 \rightarrow B}$. Another is $k_{C2 \rightarrow D2} \sim k_{B2 \rightarrow B}$, $k_{C2 \rightarrow I}$ and the different temperature dependence of $k_{C2 \rightarrow D2}$ from those of $k_{C2 \rightarrow B}$ and $k_{C2 \rightarrow I}$, if we assume that $k_{C2 \rightarrow D2}/k_{C2 \rightarrow B}$ is independent of temperature. The energy barrier between F_i and C_2 which was presumed by Hurley et al. (1977) is not necessary for the appearance of the temperature dependence of $\gamma_{I \rightarrow B}$. The reaction scheme of Figs. 7 and 8 are consistent with the one which was used in the kinetic analysis of the photoconversion among R, B, and I (Kakitani and Kakitani, 1978). The only difference is the inclusion of the reaction path to I′ in the present study. This will, however, little affect the previous analysis because I′ is hardly attained from B or I. According to the result of its kinetic analysis, a is very small ($\sim$ 0.08). From Eqs. (18) and (19)

$$\gamma_{R \rightarrow B} + \gamma_{B \rightarrow R} \simeq 1, \tag{21}$$

and from Eqs. (12)–(15)

$$\gamma_{I \to B} + \gamma_{B \to I} \simeq \gamma_{I \to B} < 1 , \tag{22}$$

$$\gamma_{I' \to B} + \gamma_{B \to I'} \simeq \gamma_{I' \to B} < 1 . \tag{23}$$

Using the relation of Eq. (21), Rosenfeld et al. (1977) suggested the existence of the thermally barrierless common state in the excited state. So that, the minimum C_1 should be called the common state between F_r and F_b. On the other hand, the quantities $\gamma_{I \to B} + \gamma_{B \to I}$ and $\gamma_{I' \to B} + \gamma_{B \to I'}$ are less than one. However, the photoconversion mechanisms through C_2 and C_3 are quite similar to that through C_1. So that we should like to call C_2 and C_3 as the common states between F_i and F_b and between $F_{i'}$ and F_b, respectively.

Interaction Energies at Other Temperatures

As we noted before, the energy surface of E^I is dependent upon the temperature. This is chiefly because the protein conformation corresponding to the intermediate state changes with the temperature. At a temperature of around −70° C, lumirhodopsin is stable. Then, the energy surface of E^I is changed from Fig. 3 so that the total energy surface E^T may have three minima at the torsional angles corresponding to R, I, and L in Table 1. The result is shown in Fig. 9a. From this it is found that one valley is parallel to the θ_{11-12}-axis.

At this point we should mention that our total energy surface does not have two minima corresponding to B and L in the *trans* regions of θ_{9-10} and θ_{11-12} but has

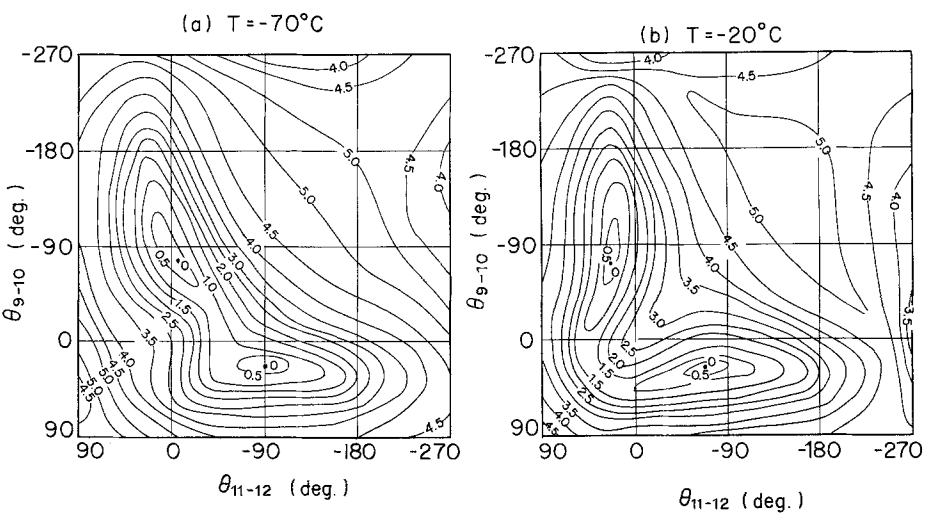

Fig. 9. The interaction energy surface E^I at (**a**) $T = -70°$ C and (**b**) $T = -20°$ C projected onto the $\theta_{9-10} - \theta_{11-12}$ plane. The left (right) energy map is estimated by the trial and error method so that the energy surface of $E^I + E^C$ in the ground state may have minima corresponding to R, L, and I (R, M, and I) at the torsional angles listed in Table 1. Energy contour unit is eV

Table 3. The calculated energies of E^C, E^I, and E^T for R, I, B, L, and M. Unit is eV

	R	I	B	L	M
E^C [a]	0	−0.1	0.9	0.4	0.1
E^I [a]	0	0.1	−0.1	0.3	0.5
E^T	0	0	0.8	0.7	0.6

[a] Origin of energy is taken to be that for R

only one minimum at each temperature. In our description, one minimum of the intermediate state changes its electronic and conformational character with the temperature. The drastic conformational change in the intermediate state can arise through the drastic changes in E^E and E^S with temperature. Even at −70° C, B will be formed at the early stage of the photoreaction from R using the similar energy surface to Fig. 7. However, this species and its energy surface are unstable and soon transform to L and the energy surface in the thermal equilibrium (Fig. 9a), respectively.

Similarly at $T \simeq -20°$ C, metarhodopsin I is stable. Thus, E^I should be chosen so that E^T may have three minima at the torsional angles corresponding to R, I, and M in Table 1. The result is shown in Fig. 9b. In this diagram it is seen that one valley is almost parallel to the θ_{11-12}-axis and the other valley to the θ_{9-10}-axis. This means that the interaction energy E^I assists to rotate only one of the two double bonds 9—10 and 11—12.

Energy Levels

According to Fig. 4, the energy levels of R, B, and I are 1.8, 2.6, and 1.8 eV, respectively. That is, the energy of B is larger than those of R and I by 18 kcal/mol. This result is consistent with an estimation of >14 kcal/mol by Rosenfeld et al. (1977). In Table 3, we listed the relative energies of E^C, E^I, and E^T for these pigments and intermediate. From this listing it is found that the interaction energy E^I is almost the same for R, I, and B but that the chromophore energy E^C of B is much larger than those of R and I. That is, the high energy in B is stored in the twisted conformation of the chromophore. A similar analysis of the energy distribution was made for L and M. The result is also listed in Table 3. From this listing, it is found that if E^T of R is assumed to be the same for each temperature, E^T's of M and L are only a little smaller than that of B. However, in these cases the mechanism by which the energy is stored differs from the case of B. In L, the large energy is stored in both E^C and E^I, and in M, the large energy is stored mainly in E^I. These facts would mean that the absorbed photon energy is first stored in the chromophore as in B then some energy is dispersed into the protein as in M. Those energy levels are drawn in Fig. 10 together with those of the excited state. In this figure it should be noticed that the energy levels of R for $T = -190°$ C, −70° C, and −20° C are set equal. In the figure the estimated levels of 11-*cis* retinal + opsin (11 + O), 9-*cis* retinal + opsin (9 + O)

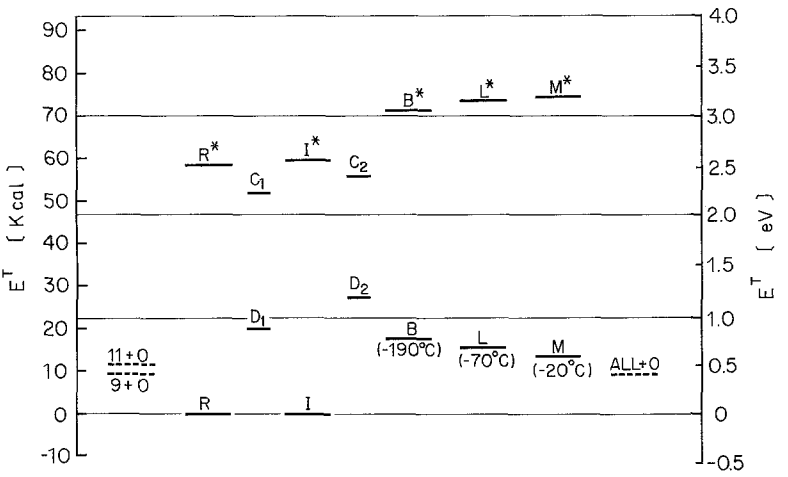

Fig. 10. Energy levels of R, I, B, L, and M together with the transition state D_1 and D_2 and the dissociated states 11 + O, 9 + O, and ALL + O, where O denotes opsin, and 11, 9, and ALL mean 11-*cis* retinal, 9-*cis* retinal, and all-*trans* retinal, respectively. The starred level is the one in the excited state. C_1 and C_2 are the common states and can be considered as the excited states of D_1 and D_2, respectively

and all-*trans* retinal + opsin (ALL + O) are also drawn. These levels were estimated from the assumption that the binding constant of 11-*cis* (9-*cis*) retinal to opsin is at least 10^7 M^{-1} (Kropf et al., 1973), and that the energy level of 11-*cis* retinal is higher than those of 9-*cis* and all-*trans* retinals by 2 kcal/mol. It is also evident that the energies of B, L, M and ALL + O are decreasing successively as expected. The energy gaps between C_1 and D_1 and between C_2 and D_2 are 1.3 eV and 1.2 eV, respectively, which are much smaller than those between R and R* and between I and I*. The energy level of I′ which was not written in the figure is calculated to be higher than that of I by 4 kcal/mol.

The energy levels in Fig. 10 correspond to free energies. However, there is a close resemblance between our calculated values and enthalpis obtained from the calorimetric experiment of Cooper and Converse (1976). According to their experiments, the enthalpy change due to the transformation from R to M is 17 kcal/mol. This result almost agrees with our calculated value of 14 kcal/mol. Apparently the entropy difference is small between R and M. However, this is not so conclusive because our results should be regarded as roughly estimated ones.

Conclusion and Discussions

In this paper we have shown that most of the specific properties of the photoisomerization reaction in visual pigments can be consistently explained by the torsion model. In this analysis we have estimated the interaction energy surface E^I by use of the chromophore conformations in the ground state, and obtained the total energy surfaces of the excited state using the above interaction energy surface. It should be noticed that the property of steric hindrance interaction was used only at the point

where the same interaction energy would work for the ground and the excited states. If similar interaction energy surfaces as ours could be obtained by the other mechanism, we would not adhere to the steric hindrance mechanism. From this point of view, it is interesting to see what energy surfaces would be obtained in the charge stabilization model of Warshel (1978).

It would be valuable to provide some discussion here as to the rapid velocity of the photoreaction of visual pigments. At room temperature, the formation of bathorhodopsin from cattle rhodopsin occurs within 6 ps after illumination of light (Busch et al., 1972). We should ask whether such a fast reaction will be realized using our energy surfaces. The recent picosecond and nanosecond kinetic experiments showed that photoisomerization of 11-*cis* PRSB in solution occurred much slower ($\sim$ 10 ns) than that of rhodopsin (Huppert et al., 1977). This is due to the absence of the thermally barrierless common state for PRSB in solution. On the other hand, Teschke et al. (1977) showed that 90° twisting of the central double bond of *cis*-stilbene occurred in 7 ps after irradiation with light and it took the order of nanoseconds to relax into the *trans*-stilbene ground state. The first excited state of stilbene is believed to have a barrierless common state similar to Fig. 10. Thus, it is found that the existence of the common state is necessary but not sufficient for a fast photoisomerization. In the case of the visual pigment, the energy gap between C_1 and D_1 is small. As a result, its radiationless transition rate is expected to be large following the energy gap law (Englman and Jortner, 1970). The radiationless transitions $C_1 \rightarrow$ B and $C_1 \rightarrow$ R are also expected to be rapid because the conformation change of the chromophore between C_1 and B or R is not so large or small as to decrease the Franck-Condon factor very much. According to our preliminary calculations (Kakitani et al., 1979), those rates are $10^{11} \sim 10^{13}$ s^{-1}. The advanced calculations are in progress.

Gawinowicz et al. (1977) reported that the rhodopsin analogue formed from 11,12-dihydroretinal (11,12-2 H ret) and opsin had the absorption maximum at 345 nm which was 75 nm bathochromic shift from λ_{max} of the protonated Schiff base (PSB) of 11,12-2 H ret. It is difficult to explain its large shift by the torsion model alone. Recently Rafferty (1979) suggested that one tryptophan residue would be close to the chromophore, from the experimental analysis of the light-induced change in the UV absorption spectrum of bovine outer segment membrance. Thus, there is a possibility that one tryptophan residue is located near the conjugated part $C_{13} \ldots N_{16}$ of the chromophore. If so, λ_{max} of the above rhodopsin analogue becomes very large because the excitation resonance between the tryptophan residue and the PSB of 11,12-2 H ret is large due to the similarity of the both λ_{max}'s. On the other hand, in the case of the native pigments, the bathochromic shift due to this mechanism will not be large because the excitation resonance between the tryptophan residue and PRSB is small due to the large discrepancy in those λ_{max}'s. We expect that the torsional mechanism will be more effective than the closeness of the tryptophan residue for the large bathochromic shift of the native pigment [we are not considering that the tryptophan residue is so close to the chromophore that a considerable electronic charge transfer occurs in the excited state as suggested by Muthukumar and Weimann (1978)]. Apart from this mechanism, there is the other possibility that an ionized group is located near the conjugated part $C_{13} \ldots N_{16}$ of the chromophore so that the π-electron delocalization of the above rhodopsin analogue

is enhanced (Honig, private communication). Even in this case, we expect that the ionized group will play only a subsidiary role to the bathochromic shift of the native pigment. If either or both of these supplemental mechanisms do play some role in the bathochromic shift of visual pigments and photoproducts, the torsional angles listed in Table 1 should be reduced to some extent. Those theoretical analyses are in progress.

Our next problem is to investigate by what mechanism the energy surface of E^I which was empirically obtained in this study can be realized. We have an idea that the necessary energy which compensates the large twisting energy ($0.5 \sim 1$ eV) stored in the chromophore would be supplied by the hydrophobic bonding effect among opsin, chromophore and the solvent. This study is in progress.

Acknowledgements. The author wishes to thank Prof. S. Yomosa, Dr. H. Kakitani, and Mr. A. Sarai for their helpful advice. Thanks are due to Prof. T. Yoshizawa and Dr. S. Kawamura with whom the author has discussed the specific reaction paths. This manuscript was much improved by the referees' critical comments.

References

Aton, B., Doukas, A. G., Callender, R. H., Becher, B., Ebrey, T. G.: Resonance Raman studies of the purple membrane. Biochemistry **16,** 2995–2999 (1977)

Busch, G. E., Applebury, M. L., Lamola, A. A., Rentzepis, P.: Formation and decay of prelumirhodopsin at room temperatures. Proc. Natl. Acad. Sci. USA **69,** 2802–2806 (1972)

Callender, R., Honig, B.: Resonance Raman studies of visual pigments. Ann. Rev. Biophys. Bioeng. **6,** 33–55 (1977)

Cooper, A., Converse, C. A.: Energetics of primary processes in visual excitation: photocalorimetry of rhodopsin in rod outer segment membranes. Biochemistry **15,** 2970–2978 (1976)

Englman, R., Jortner, J.: The energy gap law for radiationless transition in large molecules. Mol. Phys. **18,** 145–164 (1970)

Gawinowicz, M. A., Balogh-Nair, V., Sabol, J. S., Nakanishi, K.: A nonbleachable rhodopsin analogue formed from 11,12-dihydroretinal. J. Am. Chem. Soc. **99,** 7720–7721 (1977)

Huppert, D., Rentzepis, P. M., Kliger, D. S.: Picosecond and nanosecond isomerization kinetics of protonated 11-*cis* retinylidene Schiff bases. Photochem. Photobiol. **25,** 193–197 (1977)

Hurley, J. B., Ebrey, T. G., Honig, B., Ottolenghi, M.: Temperature and wavelength effects on the photochemistry of rhodopsin, isorhodopsin and their photoproducts. Nature **270,** 540–542 (1977)

Jortner, J.: Temperature dependent activation energy for electron transfer between biological molecules. J. Chem. Phys. **64,** 4860–4867 (1976)

Kakitani, T.: Theoretical study of optical absorption curves of molecules. IV. Improvement of self-consistent HMO method using a new resonance integral and investigation of a relation between bond alternation and wavelength of optical absorption. Prog. Theor. Phys. **52,** 1721–1736 (1974)

Kakitani, T., Kakitani, H.: Molecular mechanism for the initial process of visual excitation. I. Model of photoisomerization in rhodopsin and its theoretical basis by a quantum mechanical calculation of adiabatic potential. J. Phys. Soc. Jpn. **38,** 1455–1463 (1975)

Kakitani, T., Kakitani, H.: Application of self-consistent HMO theory to heteroconjugated molecules. Theor. Chim. Acta **46,** 259–275 (1977)

Kakitani, T., Kakitani, H.: Mechanism of photoconversion among rhodopsin, isorhodopsin, and bathorhodoprin. J. Phys. Soc. Jpn. **44,** 1403–1404 (1978)

Kakitani, T., Kakitani, H.: Molecular Mechanism for the initial Process of visual excitation III. Theoretical study of optical spectra and conformations of chromophores in visual pigments, analogues and intermediates based on the tortion model. Biophys. Struct. Mech. **5,** 55–73 (1979a)

Kakitani, H., Kakitani, T.: Theoretical analysis of resonance Raman spectra of rhodopsin and isorhodopsin. J. Phys. Soc. Jpn. **47,** 248–259 (1979b)

Kakitani, T., Kakitani, H., Sarai, A.: Calculation of radiationless transition rate in visual pigment. J. Phys. Soc. Jpn. (1979), submitted

Kakitani, T.: Twisting mechanism of the chromophore of visual pigment. (1979, in preparation)

Kropf, A., Hubbard, R.: The mechanism of bleaching rhodopsin. Ann. N.Y. Acad. Sci. **74,** 266–280 (1958)

Kropf, A., Whittenberger, B. P., Goff, S. P., Waggoner, A. S.: The spectral properties of some visual pigment analogs. Exp. Eye Res. **17,** 591–606 (1973)

Mathies, R., Freedman, T. B., Stryer, L.: Resonance Raman studies of the conformation of retinal in rhodopsin and isorhodopsin. J. Mol. Biol. **109,** 367–372 (1977)

Matsumoto, H., Yoshizawa, T.: Existence of a β-ionone ring-binding site in the rhodopsin molecule. Nature **258,** 523–526 (1975)

Muthukumar, M., Weimann, L. J.: On the origin of the bathochromic shift in rhodopsin. Chem. Phys. Lett. **53,**426–438 (1978)

Rafferty, C. N.: Light-induced perturbation of aromatic residues in bovine rhodopsin and bacteriorhodopsin. Photochem. Photobiol. **29,** 109–120 (1979)

Rosenfeld, T., Honig, B., Ottolenghi, M., Hurley, J., Ebrey, T. G.: *Cis*-trans isomerization in the photochemistry of vision. Pure Appl. Chem. **49,** 341–351 (1977)

Sarai, A., Kakitani, T., Shichida, Y., Tokunaga, F., Yoshizawa, T.: Kinetic analysis of photoconversion process of squid rhodopsin at liquid helium temperature. Photochem. Photobiol. (1979), submitted

Strackee, L.: Photodichroism of rhodopsin solution at −196° C. Photochem. Photobiol. **15,** 253–268 (1972)

Tarasova, N. V., Sverdlov, L. M.: Vibrational spectra of unsaturated hydrocarbons XIII. Calculation and interpretation of the vibrational spectra of trans-1,3-butadiene and trans-hexadeutero-1,3-butadience. Opt. Spectry. **18,** 336–338 (1965)

Teschke, O., Ippen, E. P., Holtom, G. R.: Picosecond dynamics of the singlet excited state of trans- and cis-stilbene. Chem. Phys. Lett. **52,** 223–235 (1977)

Warshel, A.: Charge stabilization mechanism in the visual and purple membrance pigments. Proc. Natl. Acad. Sci. USA **75,** 2558–2562 (1978)

Received November 6, 1978/Accepted March 29, 1979